Iranian Journal of Medical Physics

ijmp.mums.ac.ir

Monte Carlo-Based Microdosimetry Analysis of a Mono-energetic 330 MeV/u Carbon Ion Beam for Predicting the Relative Biological Effectiveness of Carbon Ion Therapy

M. Arif Efendi[1*], Indra Oktafian[1], Aldino Putra Andeaz[1], Valerie Valencia[1], Ying Chee Keat[2], Bukhoree Sahoh[3]

1. Department of Nuclear Engineering and Engineering Physics, Faculty of Engineering, Universities Gadjah Mada, Indonesia
2. Department of Biomedical Imaging, Pusat Kanser Tun Abdullah Ahmad Badawi, University Sains Malaysia, Malaysia
3. School of Informatics, Walailak University, Thailand and Informatics Innovation Center of Excellence (IICE), Walailak University, Thailand

ARTICLE INFO

Article type:
Original Paper

Keywords:
Bragg Peak
Carbon Ion Therapy
Microdosimetry
Monte Carlo Simulation
Relative Biological Effectiveness

ABSTRACT

Introduction: Accurate prediction of Relative Biological Effectiveness (RBE) is critical for carbon ion radiotherapy due to the strong variation of biological response along the beam path. Microdosimetric modeling provides a physics-based approach to estimate RBE by characterizing microscopic energy deposition. This study aims to evaluate the RBE at a 10% survival fraction (RBE_{10}) for a mono-energetic 330 MeV/u carbon ion beam using Monte Carlo-based microdosimetric analysis.

Material and Methods: Monte Carlo calculations were conducted using the TOol for PArticle Simulation (TOPAS) incorporating microdosimetric extension. A mono-energetic 330 MeV/u carbon ion beam traversing a water phantom was modeled, with a three-dimensional silicon-on-insulator (SOI) Bridge microdosimeter embedded in the geometry to record microdosimetric energy deposition. Microdosimetric spectra were obtained at various depths, and the dose-mean lineal energy ($\overline{yD}$) was calculated. The modified Microdosimetric Kinetic Model (MKM) with Human Salivary Gland (HSG) cell parameters was applied to estimate RBE_{10} along the beam path.

Results: The simulation predicted the Bragg peak at 201 mm, closely matching the experimental result with a deviation of approximately 2.8 mm. The $\overline{yD}$ increased markedly toward the Bragg peak region, reflecting enhanced linear energy transfer. The calculated RBE_{10} increased from approximately 1.17 at the beam entrance to a maximum of 3.02 ± 0.38 at a depth of 201 mm, corresponding to the Bragg peak, followed by a gradual decrease beyond this region.

Conclusion: Monte Carlo-based microdosimetric modeling using an SOI microdosimeter and modified MKM provides a feasible approach for estimating RBE_{10} distributions in carbon ion therapy. This approach is valuable for biological dose assessment and optimization of treatment planning.

► *Please cite this article as:*
Efendi MA, Oktafian I, Andeaz AP, Valencia V, Keat YC, Sahoh B. Monte Carlo-Based Microdosimetry Analysis of a Mono-energetic 330 MeV/u Carbon Ion Beam for Predicting the Relative Biological Effectiveness of Carbon Ion Therap. Iran J Med Phys 2026; 23 (3): 155-161. 10.22038/ijmp.2026.94089.2679.

Introduction

Cancer continues to pose a major burden on global public health. Data from the World Health Organization indicate that cancer was responsible for approximately 10 million deaths worldwide in 2022.[1] Earlier estimates from the GLOBOCAN 2020 database reported around 19.3 million newly diagnosed cancer cases and approximately 10 million cancer-related deaths across 185 countries. Furthermore, the global cancer burden is expected to increase substantially, potentially reaching about 28 million new cases each year.[2]

This increasing trend is strongly related to aging populations, unhealthy lifestyles, and environmental risk factors.[3] Despite great progress in treatment, standard approaches such as surgery, chemotherapy, and photon-based radiotherapy still face big limitations. Surgery may not be an option for tumors located near vital organs, chemotherapy often causes severe side effects and drug resistance, and photon radiotherapy distributes energy along its entire path, exposing normal tissue and increasing risks of late complications.[4,5] These challenges highlight the urgent need for more precise and biologically powerful treatment options.

Particle therapy offers a promising alternative. Unlike photons, protons and carbon ions deliver dose through the Bragg peak, concentrating maximum energy inside the tumor and sparing surrounding tissues.[6] While protons improve spatial precision, their RBE is close to 1.1, providing a limited biological

*Corresponding Author: Tel: +6282226905440; Email: arif.e@ugm.ac.id

advantage.[7] Carbon ions, however, are high Linear Energy Transfer (LET) particles that produce dense ionization tracks, leading to complex DNA damage that is difficult for tumor cells to repair. This makes them highly effective against hypoxic and radioresistant tumors, which are often resistant to conventional therapy.[8]

Biological effectiveness in carbon ion therapy cannot be fully described by absorbed dose alone. Microdosimetry provides a more detailed characterization by studying stochastic patterns of energy deposition in volumes comparable to cell nuclei. It introduces quantities such as frequency-mean lineal energy ($\overline{y_F}$) and dose-mean lineal energy ($\overline{y_D}$), which provide insights into radiation quality.[5], [10] These parameters directly link physical energy deposition to biological outcomes and are widely used in predictive models such as the Microdosimetric Kinetic Model (MKM).[10]

Traditionally, microdosimetry was performed using tissue-equivalent proportional counters (TEPCs), which are large and unsuitable for clinical application.[5] Advances in semiconductor technology led to the development of SOI microdosimeters, which are compact, highly sensitive, and capable of simulating cell-sized sensitive volumes (SVs).[11] Variants such as Bridge SOI[12–14] and Mushroom SOI[15–17] microdosimeters have been successfully validated against Monte Carlo simulations and experimental data, demonstrating their potential for clinical quality assurance.

The biological effectiveness of carbon ion therapy is generally expressed in terms of the RBE, which is defined as the ratio of the photon dose to the carbon ion dose required to achieve an equivalent biological effect.[18] In contrast to protons, which exhibit a nearly constant RBE of about 1.1, the RBE of carbon ions varies substantially depending on LET, tissue radiosensitivity, and depth along the beam path.[19,20] Both experimental and clinical evidence indicate that RBE values typically range from 2 to 4 in the region of the Bragg peak, where LET is maximized, and complex DNA lesions are most pronounced.[4,5] This variability represents both a therapeutic advantage, by increasing tumor control probability, and a challenge, due to the elevated risk of normal tissue complications if RBE is not accurately modeled. To address this, recent research has focused on refining predictive approaches using modified MKM, in addition to the development of microdosimetry-informed biological weighting functions, which have been validated through Monte Carlo simulations and in vitro cell survival experiments.

Although clinical carbon ion radiotherapy is typically delivered using Spread-Out Bragg Peak (SOBP) fields, the present study intentionally employed a mono-energetic 330 MeV/u carbon ion beam. The use of a mono-energetic beam provides a simplified and controlled environment for evaluating the intrinsic relationship between microdosimetric quantities and biological effectiveness without the additional complexity introduced by energy modulation. This approach enables direct validation of the TOPAS microdosimetric extension, the 3D SOI Bridge microdosimeter model and the modified MKM. Therefore, this work should be regarded as a baseline physical and biological validation study that establishes the foundation for future investigations involving clinically realistic SOBP configurations and patient-specific geometries.

Materials and Methods

Monte Carlo Simulation

All calculations were performed using TOPAS version 3.9, a Monte Carlo code built on the Geant4 toolkit and commonly adopted in particle-therapy research to track charged-particle transport along with the associated energy deposition and nuclear interaction processes in tissue-equivalent materials.[21,22] Micron-scale energy deposition was resolved by pairing the TOPAS microdosimetric extension with a model of the 3D SOI Bridge Microdosimeter, a detector design first developed at the Centre for Medical Radiation Physics (CMRP), University of Wollongong (UOW), Australia.[23]

The primary particle source consisted of fully ionized carbon-12 ions (12C6+) with a total kinetic energy of 3960 MeV, corresponding to 330 MeV/u. An energy spread of 0.1% was applied to approximate realistic beam conditions. The beam was directed along the positive z-axis toward a homogeneous water phantom with dimensions sufficient to encompass the complete particle range and distal fragmentation region.

The depth–dose distribution was scored using 301 bins along the beam direction, corresponding to a spatial resolution of approximately 1 mm per voxel. The simulated Bragg peak position was subsequently compared with the experimental measurements reported by Sihver et al. [24] for validation of the physical beam model.

The physics constructor list used was g4em-standard_opt4, g4h-phy_QGSP_BIC_HP, g4stopping, g4em-extra, g4h-elastic_HP, g4ion-binarycascade, g4radioactivedecay, and g4decay. These physics models have been extensively validated for heavy-ion transport simulations and are commonly employed in carbon ion therapy research.

For the macroscopic depth–dose calculation, 10^5 primary carbon ions were transported through a water phantom to obtain the Bragg curve, which was validated against published experimental data.[24] For the microdosimetric simulations, the number of histories of 10^5, 10^6, and 10^7 were employed in the plateau, Bragg peak, and tail regions, respectively, to ensure adequate statistical accuracy in the energy deposition spectra.

Microdosimetric Spectra

For the mono-energetic 330 MeV/u carbon ion beam, microdosimetric spectra were generated to

characterize microscopic energy-deposition patterns along the beam path in a water phantom. These spectra represent the probability distribution of lineal energy. This is expressed mathematically as Equation 1. Where ε is the energy imparted in a site, and l is the mean chord length of the SV.

$$y = \frac{\epsilon}{l} \quad (1)$$

The simulations were performed using the 3D SOI Bridge Microdosimeter geometry implemented in the TOPAS microdosimetric extension. This detector consists of micrometer-scale silicon SV designed to emulate the dimensions of biological targets and enable measurement of energy deposition events at cellular length scales.[23] From the spectra, the frequency-mean lineal energy ($\overline{y_F}$) and dose-mean lineal energy ($\overline{y_D}$) were extracted using the following definitions in Equation 2 and Equation 3.

$$\overline{y_F} = \int_0^\infty y f(y) dy \quad (2)$$

and

$$\overline{y_D} = \int_0^\infty y d(y) dy \quad (3)$$

where $f(y)$ and $d(y)$ represent the frequency and dose probability density functions, respectively.

The $\overline{y_F}$ characterizes the average energy deposition event, whereas the $\overline{y_D}$ emphasizes high-energy deposition events and is therefore more closely related to biological effectiveness. Consequently, $\overline{y_D}$ serves as a key input parameter in microdosimetry-based radiobiological models.

RBE_{10} Calculation

In this study, the RBE_{10} for a mono-energetic 330 MeV/u carbon ion beam was estimated using the modified MKM. The model links the dose mean lineal energy ($\overline{y_D}$) obtained from Monte Carlo-based microdosimetric spectra to the linear quadratic (LQ) parameters of the photon reference radiation. According to the modified MKM, the relationship can be expressed as Equation 4.

$$RBE_{10} = \frac{2\beta_{ref} D_{10,ref}}{\sqrt{\alpha_p^2 - 4\beta_{ref} \ln(0.1)} - \alpha_p} \quad (4)$$

This formulation has been widely applied in carbon ion therapy RBE modeling, as demonstrated in both experimental and simulation studies [8], [9], [19].

The modified MKM requires biological and geometrical parameters corresponding to a reference cell line. In this study, the HSG tumor cell line was adopted, following the original implementation of the MKM in carbon-ion radiotherapy studies. The parameters used were α_0 = 0.13 Gy-1, β = 0.05 Gy-2, domain radius rd = 0.42 µm, and nuclear radius Rn = 6 µm. The reference radiation was 200 kVp X-rays with αX = 0.19 Gy^{-1} and βX = 0.05 Gy^{-2}. These parameters were employed to convert the simulated $\overline{y_D}$ into the corresponding RBE_{10} values.

Parameter	Value
Cell line	HSG
α_0	0.13 Gy-1
y0	150 keV/µm
β	0.05 Gy-2
ρ	1 g/cm³
rd	0.42 µm

3D SOI Bridge Microdosimeter Geometry

The microdosimetric calculations were performed using the 3D SOI Bridge Microdosimeter implemented within the TOPAS Microdosimetric Extension developed by Zhu *et al* [23]. The simulated detector configuration replicates the SOI Bridge microdosimeter developed by the CMRP, UOW. The SV consists of a grid of 59 rows and 72 columns, with each SV consisting of a silicon block measuring 30 × 30 × 10 µm³, with neighboring SVs interconnected through a silicon bridge measuring 20 × 15 × 10 µm³, placed on a 300 µm-thick supporting silicon substrate with an upper 1 µm-thick SiO_2 insulation layer. For this detector configuration, the mean path length (l) used as the denominator in Equation 1 was assumed to be 10 µm, corresponding to the thickness of the silicon layer in the SV. This value follows the methodology established by Zhu *et al.* [23], who demonstrated that the conventional Cauchy mean-chord-length formula does not directly apply to the Bridge SOI geometry due to its non-isotropic SV structure, and is consistent with the Mean Path Length parameter specified in the TOPAS microdosimetric scorer used in this study. The detector model, material composition, silicon-to-water conversion methodology, and lineal energy scoring procedures were implemented according to this validated framework.

Results

Depth-Dose Distribution

Figure 1 presents the depth-dose distribution of the mono-energetic 330 MeV/u carbon ion beam in water. The simulated Bragg peak was observed at a depth of 201.00 mm, whereas the corresponding experimental value reported by Sihver *et al.*[24] occurred at 198.19 mm. The resulting range difference was 2.81 mm.

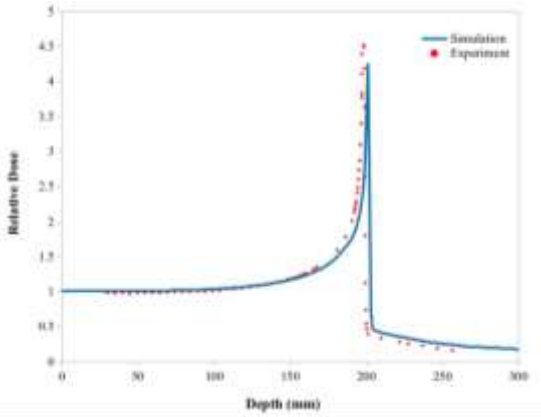


Figure 1. Depth Dose Profile of a mono-energetic 330 MeV/u Carbon Ions in Water

Microdosimetric Spectra

Representative microdosimetric spectra obtained at various depths are shown in Figure 2. The spectra progressively shifted toward larger lineal energy values as the beam penetrated deeper into the phantom. The largest contribution of high-lineal-energy events occurred near the Bragg peak region, indicating increased microscopic energy deposition density.

Dose-Mean Lineal Energy Distribution

The depth dependence of dose-mean lineal energy $\overline{yD}$ is illustrated in Figure 3. The $\overline{yD}$ values remained relatively low throughout the entrance region, ranging from approximately 12 to 20 keV/µm. A rapid increase was observed near the Bragg peak, where the maximum $\overline{yD}$ value reached approximately 272 keV/µm, occurring at 202 mm. Past the Bragg peak, $\overline{yD}$ decreased gradually but remained elevated compared with the entrance region due to the presence of secondary fragments.

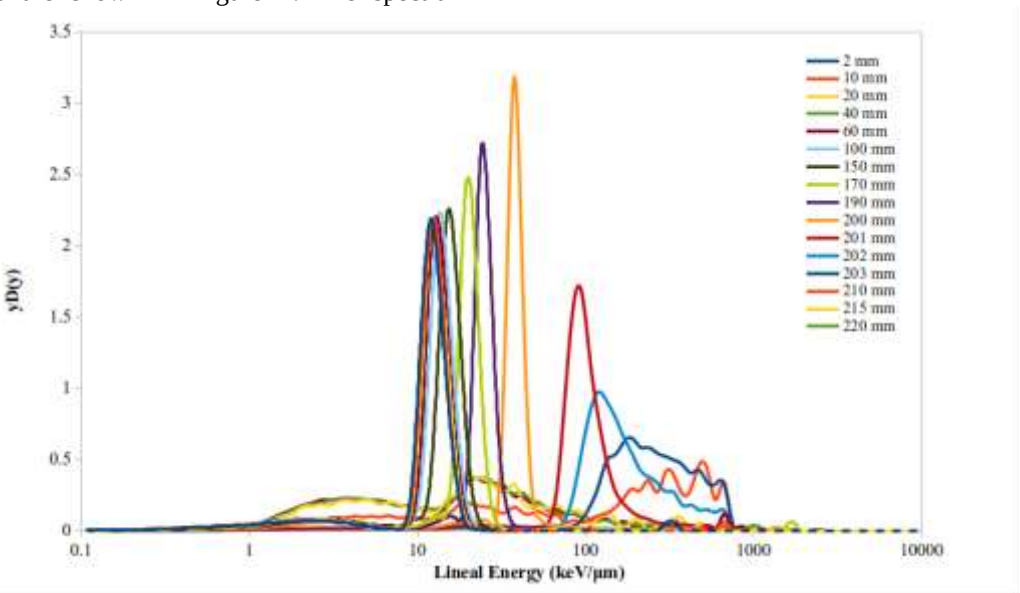


Figure 2. Lineal Energy Spectra of a mono-energetic 330 MeV/u Carbon Ions in Water

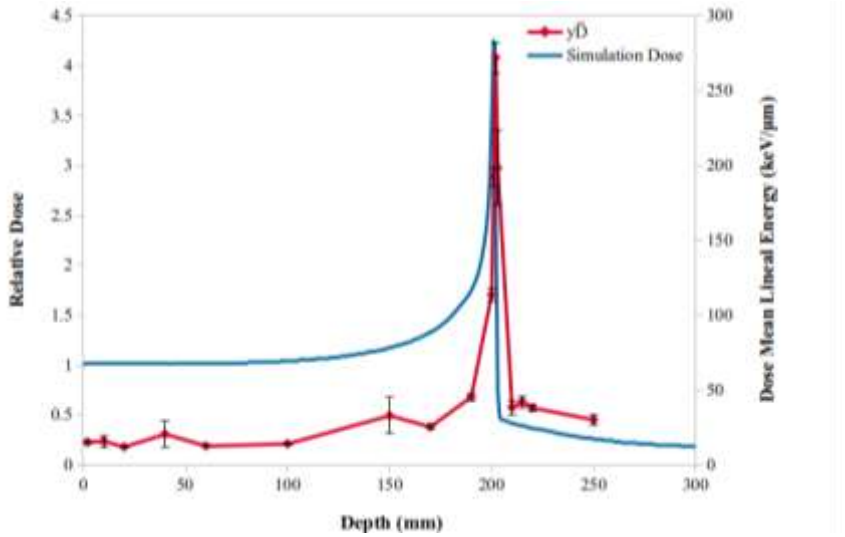


Figure 3. Dose mean lineal energy distribution as a function of depth

RBE$_{10}$ Distribution

The calculated RBE_{10} values are presented in Figure 4 and Table 1. At shallow depths, RBE_{10} remained nearly constant around 1.16–1.21. The RBE_{10} increased progressively with penetration depth and reached a maximum value of 3.02 ± 0.38 at 201 mm, corresponding to the simulated Bragg peak position.

Beyond the Bragg peak, RBE_{10} gradually decreased but remained higher than the entrance value. At depths of 202 mm and 203 mm, RBE_{10} values of 2.76 ± 0.44 and 2.06 ± 0.48 were obtained, respectively. The persistence of elevated RBE_{10} beyond the peak region indicates the continued biological contribution of secondary fragments generated through nuclear interactions.

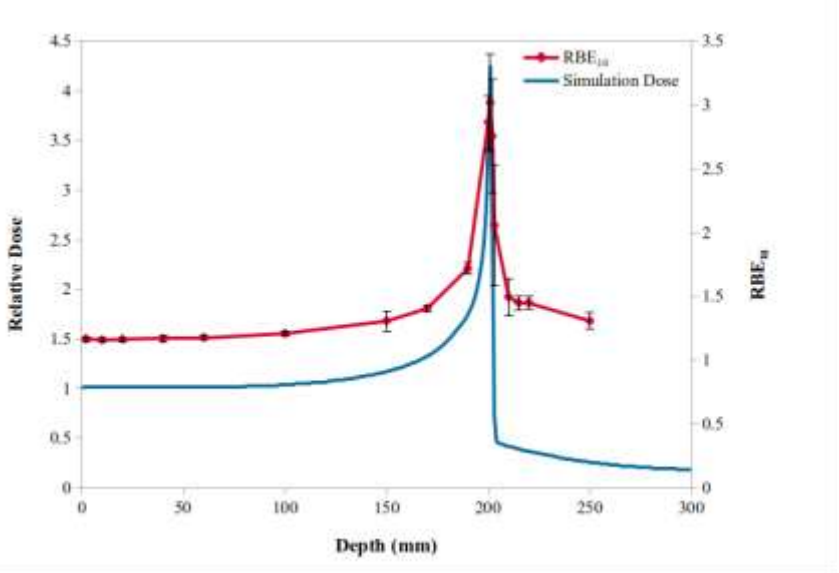


Figure 4. RBE_{10} distribution as a function of depth

Table 1. $\overline{y_F}$, $\overline{y_D}$, and RBE_{10} value of the incident 330 MeV/u carbon ion beam on the 3D SOI Bridge microdosimeter

Depth (mm)	$\overline{y_F}$ (keV/μm)	$\overline{y_D}$ (keV/μm)	RBE_{10}
2	5.17 ± 0.13	15.05 ± 1.35	1.17 ± 0.02
10	5.02 ± 0.12	15.73 ± 3.91	1.16 ± 0.02
20	5.08 ± 0.10	11.92 ± 0.37	1.16 ± 0.01
40	5.13 ± 0.12	20.43 ± 9.07	1.17 ± 0.02
60	5.08 ± 0.11	12.55 ± 0.36	1.18 ± 0.01
100	5.44 ± 0.12	13.93 ± 0.49	1.21 ± 0.02
150	6.90 ± 0.14	32.83 ± 11.99	1.31 ± 0.07
170	8.32 ± 0.09	25.29 ± 1.18	1.41 ± 0.02
190	12.74 ± 0.16	45.29 ± 2.19	1.72 ± 0.05
200	32.25 ± 0.35	113.51 ± 4.10	2.87 ± 0.21
201	46.69 ± 0.83	192.21 ± 5.97	3.02 ± 0.38
202	42.07 ± 1.15	272.14 ± 10.22	2.76 ± 0.44
203	10.68 ± 0.63	198.43 ± 24.97	2.06 ± 0.48
210	5.04 ± 0.21	38.30 ± 4.82	1.50 ± 0.15
215	4.70 ± 0.07	41.95 ± 4.19	1.45 ± 0.05
220	4.52 ± 0.06	38.00 ± 2.47	1.45 ± 0.05
250	3.11 ± 0.07	30.03 ± 3.59	1.31 ± 0.06

Discussion

The depth-dose distribution of the mono-energetic 330 MeV/u carbon ion beam in a water phantom is shown in Figure 1. The Bragg curves of the blue solid line and red dotted line are obtained using TOPAS simulation and published experimental data,[24] respectively. The simulated Bragg peak occurs at 201.00 mm, slightly deeper than the experimental Bragg peak at 198.19 mm. This 2.81 mm discrepancy is more appropriately interpreted as a systematic range shift rather than a statistical fluctuation. Such deviations may arise from uncertainties in stopping power calculations, beam energy calibration, or the physical interaction models implemented in Monte Carlo transport. Since the location of the Bragg peak determines where the highest dose is delivered, accurate range prediction is essential for reliable biological effectiveness estimation

The spectra in Figure 2, plotted at successive depths, shift toward higher lineal energy as the beam advances into the phantom, an effect most pronounced close to the Bragg peak. This is consistent with the rise in LET that accompanies the ions slowing down near the end of their range. Near the Bragg peak, high-linear-energy events make up a growing share of the spectrum, pointing to denser energy deposition within the detector's SV. Because such deposition patterns tend to produce more complex DNA damage, this shift helps explain the rise in biological effectiveness seen toward the distal end of the beam. Figure 3 tracks $\overline{y_D}$ as a function of depth. Its rise from the entrance region toward the Bragg peak mirrors the gradual slowing of the primary carbon ions and the accompanying increase in LET, with the peak $\overline{y_D}$ value occurring where the ions release most of their remaining energy. Beyond the Bragg peak, $\overline{y_D}$ decreases because the primary carbon ions have largely stopped and the radiation field becomes increasingly dominated by secondary fragments. This trend confirms that the microdosimetric quantities obtained from the SOI microdosimeter are consistent with the expected physical behavior of carbon ion beams in water.

Figure 4 presents the depth-dependent RBE_{10} values calculated using the modified MKM. The RBE_{10} distribution follows a similar trend to that observed for $\overline{y_D}$, increasing gradually with depth and reaching its maximum near the Bragg peak. This behavior demonstrates the strong dependence of biological effectiveness on radiation quality.

The elevated RBE_{10} values around the Bragg peak region indicate that carbon ion therapy provides enhanced biological effectiveness precisely where the highest physical dose is delivered. Such a characteristic is advantageous for tumor control because it combines favorable dose localization with increased biological damage. In contrast, the gradual decrease in RBE_{10} beyond the Bragg peak reflects the reduced contribution of high-LET primary ions, although residual biological effectiveness remains due to secondary fragments produced through nuclear interactions.

Table 1 tabulates $\overline{y_F}$, $\overline{y_D}$, and RBE_{10} along the penetration depth passed by the mono-energetic 330 MeV/u carbon ion beam. The coincidence of the maximum $\overline{y_D}$ and maximum RBE_{10} near the Bragg peak demonstrates the close relationship between microdosimetric quantities and biological effectiveness. This observation supports the use of microdosimetric measurements combined with the modified MKM framework for estimating RBE in carbon ion therapy.

However, because the simulated Bragg peak position differs from the experimental reference by 2.81 mm, the corresponding biological effectiveness peak is also shifted. This result highlights the importance of accurate beam range modeling, since uncertainties in the physical dose distribution directly affect the predicted location of maximum biological effectiveness.

Conclusion

This study demonstrated the feasibility of combining Monte Carlo-based microdosimetry with the modified MKM to estimate RBE_{10} distributions for a mono-energetic 330 MeV/u carbon ion beam in water. The simulated microdosimetric spectra, dose-mean lineal energy distributions, and RBE_{10} profiles exhibited the expected increase toward the Bragg peak, with a maximum RBE_{10} value of 3.02 ± 0.38 obtained at a depth of 201 mm.

While the overall physical and biological trends were consistent with established carbon ion therapy behavior, a systematic Bragg peak range difference of 2.81 mm and elevated uncertainties in the Bragg peak and fragmentation-tail regions were observed. A further limitation is evident in the statistical uncertainty of the fragmentation tail region, where the relative uncertainty in RBE_{10} reached approximately 23% at 203 mm (RBE_{10} = 2.06 ± 0.48) despite the use of 10^7 histories. This reflects a well-known limitation of standard analog Monte Carlo simulation when tracking rare secondary fragmentation events. These findings indicate that further refinement and validation of the simulation framework are required, and future work should consider variance reduction techniques, such as geometrical splitting or Russian roulette, to improve statistical precision in this distal tail region without proportionally increasing computational cost.

Therefore, the present work should be regarded as a proof-of-concept and baseline validation study demonstrating the capability of TOPAS-based microdosimetry for biological effectiveness estimation. Future work should extend the methodology to clinically relevant SOBP beams, heterogeneous anatomical geometries, and larger simulation statistics before integration into a treatment planning system.

Acknowledgment

The authors gratefully acknowledge Universitas Gadjah Mada for providing the institutional support necessary to complete this research. This work was funded by the DTNTF Research Grant Program 2025.

References

1. Bray F, Laversanne M, Sung H, Ferlay J, Siegel RL, Soerjomataram I, et al. Global cancer statistics 2022: GLOBOCAN estimates of incidence and mortality worldwide for 36 cancers in 185 countries. CA Cancer J Clin. 2024 [cited 2025 Nov 6];74(3):229–63.
2. Sung H, Ferlay J, Siegel RL, Laversanne M, Soerjomataram I, Jemal A, et al. Global Cancer Statistics 2020: GLOBOCAN Estimates of Incidence and Mortality Worldwide for 36 Cancers in 185 Countries. CA Cancer J Clin. 2021;71(3):209–49.
3. Bray F, Laversanne M, Weiderpass E, Soerjomataram I. The ever-increasing importance of cancer as a leading cause of premature death worldwide. Cancer. 2021 [cited 2025 Nov 6];127(16):3029–30.
4. Parisi A, Beltran CJ, Furutani KM. Clonogenic Survival RBE Calculations in Carbon Ion Therapy: The Importance of the Absolute Values of α and β in the Photon Dose-Response Curve and a Strategy to Mitigate Their Anticorrelation. Quantum Beam Sci. 2023 [cited 2025 Nov 6];7(1):3.
5. Colautti P, Magrin G, Palmans H, Cortés-Giraldo MA, Conte V. Characterizing Radiation Effectiveness in Ion-Beam Therapy Part II: Microdosimetric Detectors. Front Phys. 2020;8:550458.
6. Hirao Y, Ogawa H, Yamada S, Sato Y, Yamada T, Sato K, et al. Heavy ion synchrotron for medical use -HIMAC project at NIRS-Japan-. Nucl Physics, Sect A. 1992;538(C):541–50.
7. Ilicic K, Combs SE, Schmid TE. New insights in the relative radiobiological effectiveness of proton irradiation. Radiat. Oncol. 2018;13(1).
8. Mohamad O, Sishc BJ, Saha J, Pompos A, Rahimi A, Story MD, et al. Carbon ion radiotherapy: A review of clinical experiences and preclinical research, with an emphasis on DNA damage/repair. Cancers (Basel). 2017;9(6):1–30.
9. Parisi G, Romano F, Schettino G. Microdosimetry for hadron therapy: A state of the art of detection technology. Front. Phys. 2022;10:1035956.
10. Kase Y, Kanai T, Matsumoto Y, Furusawa Y, Okamoto H, Asaba T, et al. Microdosimetric measurements and estimation of human cell survival for heavy-ion beams. Radiat Res. 2006;166(4):629–38.
11. Rosenfeld AB. Novel detectors for silicon based microdosimetry, their concepts and applications. Nucl Instruments Methods Phys Res Sect A Accel Spectrometers, Detect Assoc Equip. 2016;809:156–70.
12. Anderson SE, Furutani KM, Tran LT, Chartier L, Petasecca M, Lerch M, et al. Microdosimetric measurements of a clinical proton beam with micrometer-sized solid-state detector. Med Phys. 2017;44(11):6029–37.
13. Bolst D, Tran LT, Chartier L, Prokopovich DA, Pogossov A, Guatelli S, et al. RBE study using solid state microdosimetry in heavy ion therapy. Radiat Meas. 2017 [cited 2025 Nov 6];106:512–8.
14. Han S, Yoo SH, Shin JI, Kim EH, Jung WG, Kim KB, et al. Study on the RBE estimation for carbon beam scanning irradiation using a solid-state microdosimeter. Med Phys. 2020 [cited 2025 Nov 6];47(2):363–70.
15. Lee SH, Mizushima K, Kohno R, Iwata Y, Yonai S, Shirai T, et al. Estimating the biological effects of helium, carbon, oxygen, and neon ion beams using 3D silicon microdosimeters. Phys Med Biol. 2021;66(4):045017.
16. Sakata D, Lee SH, Tran LT, Pan V, Nakaji T, Mizuno H, et al. Microdosimetric investigation for multi-ion therapy by means of silicon on insulator (SOI) microdosimeter. Phys Med Biol. 2022;67(21):215010.
17. Samnøy AT, Ytre-Hauge KS, Malinen E, Tran L, Rosenfeld A, Povoli M, et al. Microdosimetry with a 3D silicon on insulator (SOI) detector in a low energy proton beamline. Radiat Phys Chem. 2020 [cited 2025 Nov 6];176:109078.
18. Kim Y, Kim J, Cho S. Review of the Existing Relative Biological Effectiveness Models for Carbon Ion Beam Therapy. Prog Med Phys. 2020;31(1):1–7.
19. Jeong J, Taasti VT, Jackson A, Deasy JO. The relative biological effectiveness of carbon ion radiation therapy for early stage lung cancer. Radiother Oncol. 2020;153:265–71.
20. Choi K, Molinelli S, Russo S, Mirandola A, Fiore MR, Vischioni B, et al. Rectum dose constraints for carbon ion therapy: Relative biological effectiveness model dependence in relation to clinical outcomes. Cancers (Basel). 2020;12(1).
21. Perl J, Shin J, Schümann J, Faddegon B, Paganetti H. TOPAS: An innovative proton Monte Carlo platform for research and clinical applications. Med Phys. 2012;39(11):6818–37.
22. Faddegon B, Ramos-Méndez J, Schuemann J, McNamara A, Shin J, Perl J, et al. The TOPAS tool for particle simulation, a Monte Carlo simulation tool for physics, biology and clinical research. Phys Medica. 2020;72(November 2019):114–21.
23. Zhu H, Chen Y, Sung W, McNamara AL, Tran LT, Burigo LN, et al. The microdosimetric extension in TOPAS: Development and comparison with published data. Phys Med Biol. 2019;64(14):15pp.
24. Sihver L, Schardt D, Kanai T. Depth-Dose Distributions of High-Energy Carbon, Oxygen and Neon Beams in Water. Japanese J Med Phys. 1998;18(1):1–21.